The Astrophysical Journal, 783:20 (10pp), 2014 March 1 doi:10.1088/0004-637X/783/1/20

INDIVIDUAL ALPHA ELEMENTS, C, N, AND Ba IN EARLY-TYPE GALAXIES

Guy Worthey[1], Baitian Tang[1], and Jedidiah Serven[2]
[1] Department of Physics and Astronomy, Washington State University, 1245 Webster Hall, Pullman, WA 99164-2814, USA
[2] Bellevue College, 3000 Landerholm Circle SE, Bellevue, WA 98007-6484, USA
Received 2013 March 8; accepted 2014 January 13; published 2014 February 7

ABSTRACT

Spectral data on early-type galaxies are analyzed for chemical abundance with an emphasis on obtaining detailed abundances for the elements O and Si in addition to C, N, Na, Mg, Ca, Fe, and Ba. The abundance trends with velocity dispersion fit preconceptions based upon previous Mg conclusions, namely, that larger galaxies have a higher alpha element to iron peak ratio indicative of a higher ratio of Type II to Type Ia supernova products. The heaviest alpha elements, Ca and Ti, do not participate in this trend, although this fact does not necessarily alter the basic picture given the uncertainties in nucleosynthetic yields. Elements that likely have significant contributions from intermediate-mass stars, namely, C, N, and Ba, also gain ground relative to Fe in massive galaxies at a modest level, with the Ba conclusion uncertain from our data alone. After the velocity dispersion trend is subtracted, [M/H], [N/Fe], [Na/Fe], [Mg/Fe], and [Ca/Fe] probably have cosmic scatter, and no quantity can be shown to not have cosmic scatter.

Key words: galaxies: abundances – galaxies: stellar content – Galaxy: abundances – Galaxy: stellar content – stars: abundances

1. INTRODUCTION

In early-type galaxies, tracking the abundances of individual elements is a promising avenue to learn more about the nucleosynthetic histories of these enigmatic objects because the observed abundance pattern is the sum of the chemical enrichment over the lifetime of the galaxies whether that enrichment occurred primordially or fairly recently (Audouze & Tinsley 1976). While color–magnitude relations and line strength–magnitude relations indicated some chemical enrichment as a function of early-type galaxy luminosity or velocity dispersion (Faber 1973), attention turned to the possibility of non-lockstep heavy-element enrichment as metallicity-sensitive stellar population models were produced (Peletier 1989; Worthey et al. 1992; Davies et al. 1993; Kuntschner 2000). The earliest studies concentrated on the ratio [Mg/Fe] since the diagnostic features, Mg *b*, Fe5270, and Fe5335 (spectral absorption feature index definitions of Worthey et al. 1994), were adjacent to each other in the spectrum and thus plausibly insulated from wavelength-dependent changes in things such as the ratio of dwarf to giant stellar light or the ratio of metal-poor to metal-rich stellar light.

The elements N, Ca, Na, and Ti were soon added to the list of elements with strong spectral signatures that could plausibly be measured (Worthey 1998), and it appeared that N and Na roughly tracked Mg, while Ca stayed closer to Fe across the span of velocity dispersion, with Ti, expressed in the spectrum through TiO features, being more ambiguous. Carbon can be measured via the C_2 absorption associated with the index called either Fe4668 or, later, $C_2$4668 (Tripicco & Bell 1995). Trager et al. (1998) showed that the behavior of $C_2$4668 with velocity dispersion was intermediate between Fe and Mg features and so perhaps [C/Fe] was also increasing with galaxy velocity dispersion, but more mildly than [Mg/Fe]. The Worthey (2004) case study of M32 indicated high precision of the [C/Fe] ratio and also highlighted that, if the abundance pattern were correctly taken into consideration, a mean age would be determined with much greater confidence. [C/Fe] and [Na/Fe] were slightly elevated in M32, while [N/Fe] and [Mg/Fe] depressed, but global conclusions from one decidedly peculiar elliptical galaxy are impossible to make.

Nitrogen, oxygen, and carbon are related via molecular balancing (Tripicco & Bell 1995). The CO molecule has the highest binding energy compared to C_2 or CN, so that adding oxygen tends to decrease C_2 and CN feature strengths as less free carbon is available. Leaving O as a free parameter, however, C and N can be separately disentangled by considering the CN features in the optical blue and $C_2$4668, leading to the strong N and weak C positive trends with velocity dispersion stated above. In other words, a strong O trend with velocity dispersion could strongly alter the C and N conclusions. There is a noteworthy side story regarding the NH feature at 3360 Å that at first glance should measure N alone. Toloba et al. (2009) more than doubled the amount of observational data available for this feature and found a flat trend of the index with velocity dispersion, in stark contrast to the strong trend with CN near 4100 Å. However, Serven et al. (2011) realized that this very blue feature was being weakened by weak-lined starlight from metal-poor main-sequence stars, and also that it was being negatively affected by nearby Mg absorption. There is therefore no reason to doubt the conclusions from the optical.

Calcium, being an alpha element, albeit a heavy one, might be expected to follow magnesium. Initial indications based on the index Ca4455 that has substantial contributions from other elements and Ca4227 that is somewhat cleaner (Worthey 1998) were that Ca tracks Fe, although there was some evidence that the [Ca/Fe] zero point was incorrect (Prochaska et al. 2005). Calcium also has a very strong trio of spectral features in the red (∼8600 Å) that were analyzed by Cenarro et al. (2003, 2004) with the intriguing observation that the Ca line strengths decline with increasing galaxy velocity dispersion. A possible explanation was that the initial mass function (IMF) was becoming more dwarf-heavy among larger galaxies, though of course this could also be caused by a modest decline in Ca abundance for larger galaxies. Finally, Worthey et al. (2011) analyzed the Ca K and H features, which are not sensitive to

IMF changes, to conclude that the latter explanation, a true abundance trend, was much more likely, though modest—a few tenths in the log at most.

In terms of chemical evolution and nucleosynthesis a change in the ratio of Type Ia to Type II supernova enrichment along the mass sequence of early-type galaxies would clearly explain most of what is seen in the abundance pattern if some mechanism were identified that could vary the enrichment ratio as a function of galaxy mass or velocity dispersion. There are many proposed mechanisms (see Worthey et al. 1992; Trager et al. 1998; Thomas et al. 2003; Matteucci 1994), but three example mechanisms are (1) more rapid star formation in more massive galaxies, (2) a more top-heavy upper IMF in the star formation environments found in more massive galaxies, and (3) quicker quenching of the tail ends of star formation episodes in more massive galaxies (Worthey & Collobert 2003; Pipino & Matteucci 2004). All three would operate to boost alpha elements (C, O, Ne, Si, Ti, Ca) relative to Fe-peak elements, presuming that Type II supernovae produce that whole list. It is thought that there is more Ca ejected from Type Ia supernovae than Mg (Travaglio et al. 2004), and this might modify conclusions for Ca. Also, recently, Conroy et al. (2013) added Ba and Sr to the list of elements to consider, finding that Ba tracks Mg but either that Sr has no trend, or its trend is buried in the noise. Due to their *s*-process (Burbidge et al. 1957) origin, Ba and Sr could conceivably come from a third nucleosynthetic source: intermediate-mass stars (Busso et al. 1999 points at the 2–4 $M_{\odot}$ range for most *s*-process enrichment in the Milky Way) with a timescale of enrichment longer than that of Type II supernovae (few million years) but perhaps comparable to that of Type Ia supernovae (many hundreds of millions of years because of the necessity to form white dwarf "seeds" before detonation, though "prompt" Type Ia scenarios exist, as well; Tsujimoto & Shigeyama 2012). Carbon and N plausibly also arise mostly from intermediate-mass stars (Worthey 1998; Mattsson 2010; Bensby & Feltzing 2006; Chiappini et al. 2005, 2003), although this conclusion is not perfectly clear, even for the Milky Way environment.

Proceeding onward into the unknown, the elements Si and O are key alpha elements whose nucleosynthetic source is Type II supernovae and whose measurement should theoretically track Mg very well. Calcium and Ti are heavy alpha elements that perhaps should also follow Mg, but may, in practice, not do that. It is important to confirm the Ba result of Conroy et al. (2013) and also at least somewhat chart the behavior of O because of its pragmatic importance in being able to therefore measure N and C abundances relative to some absolute scale.

The tools this group has assembled over the years to tackle the problem are about to be overhauled, and it was judged timely to publish a snapshot of the results to date. The methods for doing so are laid out in the next section, followed by the abundance results, followed by a discussion and conclusion section.

2. METHOD

The stellar population models used follow Worthey et al. (2011) with index definitions as expanded by Serven et al. (2005) and the basic infrastructure of Worthey (1994). To briefly recap, stellar evolutionary isochrones are coupled to a stellar IMF to predict the number of stars inhabiting locations in the log L, log $T_{\rm eff}$ diagram. Fluxes are associated with each bin of stars, along with empirical estimates of the absorption feature indices.

It was planned to use newly computed isochrones based on MESA (Paxton et al. 2011) evolution for this work. These isochrones would have been sensitive to abundance changes in the same way as the spectra and it is desirable to have it so, not only for the sake of consistency, but also for the scientific exploration of how the flexible evolution would augment or attenuate the spectral signals. Technical reasons prevented the timely completion of this effort, and so we proceed with the important caveat that the mild temperature and lifetime changes seen in Dotter et al. (2007) are not carried forward in this analysis. In addition to the other shortcomings to be elucidated as we proceed, there is also the fact that the stellar evolution is assumed to be scaled-solar as the abundance mixture changes. We know enough to know that for the abundance trends themselves the underlying isochrones matter only in second order, and so it is possible to proceed, albeit with due caution in the sense that absolute age and metallicity results should be regarded as provisional because of the following logic. Worthey (1994) showed that changing the temperatures or numbers of subdivided phases of stellar evolution, for example, only cool giants, causes spectral changes that lie along the age-metallicity degeneracy direction. Happily, the abundance-change vectors seldom align with the age-metallicity vectors and so are amenable to unambiguous measurement. Bertelli et al. (1994) isochrones were used for the plots in this paper, though isochrones are swappable in our code.

Synthetic spectra are used twice: once to place the continuum, and once more to provide the spectral response to changes of abundance parameters. For this paper all spectral data and model indices are transformed to a common resolution to mimic a velocity dispersion of 300 km s^{-1}. The grid of synthetic stellar spectra was compiled from three different codes (Lee et al. 2009) at high spectral resolution and then resampled to 0.5 wavelength intervals in the range 3000–10,000 Å. A list of 23 elements was included, not all of which are used in this paper, and the Grevesse & Sauval (1998) abundance list was used as the solar mixture.

Empirical spectra are still essential for adequate spectral matching. This is illustrated in Figure 1, where three workhorse indices are plotted for stars of surface temperature between 4000 and 6000 K. The empirical fits are based on three spectral libraries (Worthey et al. 1994; Valdes et al. 2004; Sánchez-Blázquez et al. 2006) and are quite solidly established. The synthetic indices were measured from the spectra we are using to estimate spectral responses as a function of abundance change, smoothed to 200 km s^{-1} for purposes of Figure 1, and serve to illustrate why empirical spectra are still essential. There tends to be far more gravity dependence in the synthetic spectra than in real stars. This is seen even in colors (Worthey & Lee 2011). Tripicco & Bell (1995) also note that cool stars will have deeper Balmer line strengths than synthetic spectra can reproduce because of chromospheric layers that are not modeled.

The medium-resolution regime highlights weak points in the synthetic spectra that can go unnoticed at very high or very low resolution: incomplete or incorrect line lists, lack of chromospheres, and uncertainty in convection and microturbulence all contribute to considerable drift between observation and calculation. See Buzzoni et al. (2001), Chavez et al. (1995, 1996, 1997), Franchini et al. (2004a, 2004b, 2005), Gulati et al. (1993), and Tripicco & Bell (1995) for more confrontations and derived wisdom. The spectra we use reproduce stellar colors very well, but are also known to suffer from incorrect Cr line parameters in addition to the regular list of defects inherent in synthetic spectra.

In order to make models of spectral indices for stellar populations, the empirical stellar behaviors, fit with multivariate

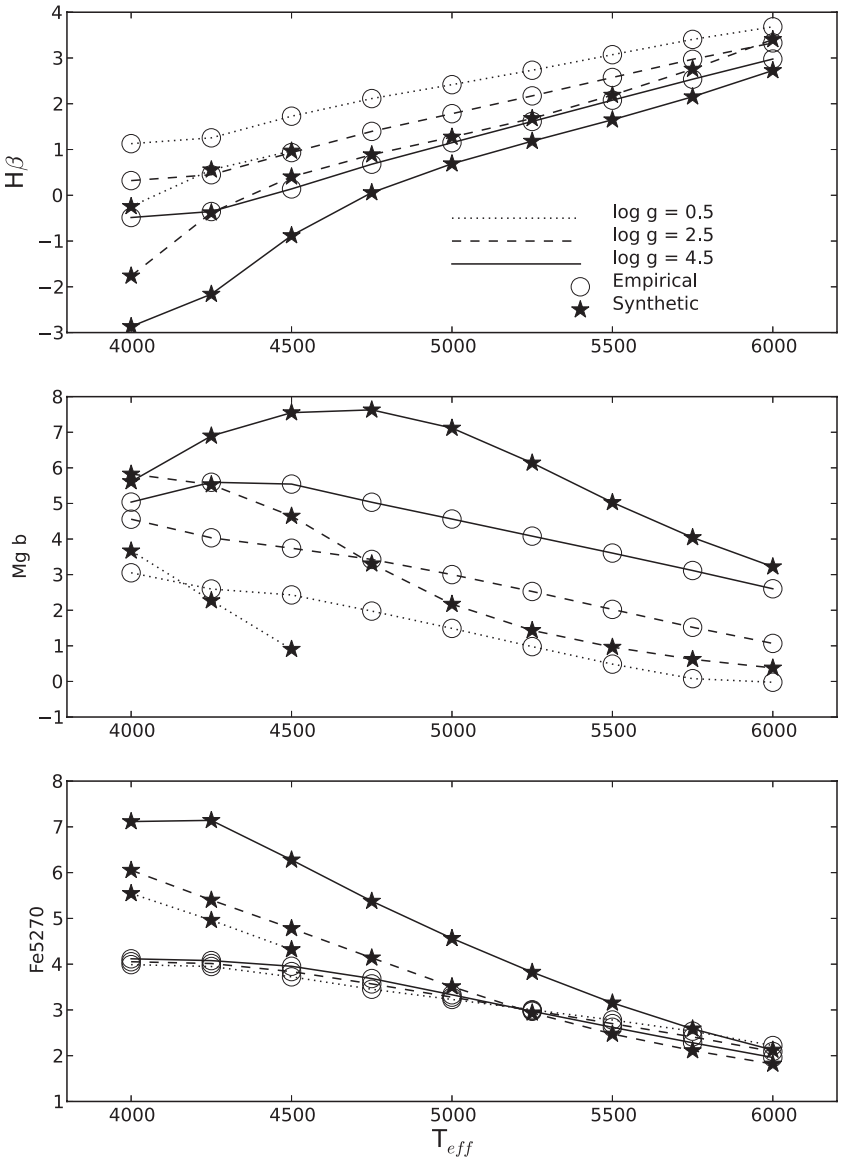

Figure 1. Hβ, Mg b, and Fe5270 indices as a function of temperature for stars. Empirical fits (open circles) are compared to index measurements from synthetic spectra (stars) for log $g = 0.5$ (dotted), 2.5 (dashed), and 4.5 (solid). Synthetic spectra show gravity dependences not seen in the observations and a weakness in Hβ that is at least partially understood as a lack of chromosphere in the model atmospheres.

polynomials and summarized in lookup tables, are used to make the basic run over populations of various ages and scaled-solar metallicities. The synthetic spectra are used in a differential sense to make indices deeper or shallower as a number of absorbers of different species come and go.

For observational material, we use spectra from Graves et al. (2007) that are grand averages of non-LINER, early-type galaxies from the Sloan Digital Sky Survey (SDSS) binned into six velocity dispersion ranges and individual galaxies from Serven (2010) that are mostly in the Virgo Cluster. Spectra and models were compared in feature-index space at a common velocity dispersion of 300 km s^{-1}. Most galaxies needed to have extra smoothing applied in order to reach this resolution, but a few of the largest galaxies needed to be corrected backward, where synthetic model spectra were used to compute the small index corrections.

An inversion program was created to find the best-fitting set of abundance parameters for a given set of indices. A single-burst age and a delta function in metallicity were used for this exercise, along with a variable number of individual elemental abundance parameters, with elements varied one by one. For ages, a collection of nine indices (HδA, HδF, HγF, Hβ, Fe4383, Fe5270, Fe5335, Na D, $C_2$4668) was used to generate a map of rms goodness of fit over the parameter range covered by the models. A smoothed map was then used to find the starting age and overall abundance. Iteratively, individual abundances were allowed to drift, and the improved chemical fingerprint carried forward to subsequent age guesses. All available indices were used in the inversion process. Index wavelength definitions come from Worthey et al. (1994), Worthey & Ottaviani (1997), and Serven et al. (2005).

No constraints were imposed on the abundance mixtures. In certain circumstances, this did indeed cause wild results, and that very wildness was used to judge when the combination of indices and index responses to the abundance changes were astrophysically meaningful. For example, Sr and Al only affect tiny portions of the spectrum at a weak level—too weak to be truly measured, so Sr and Al abundances coming from

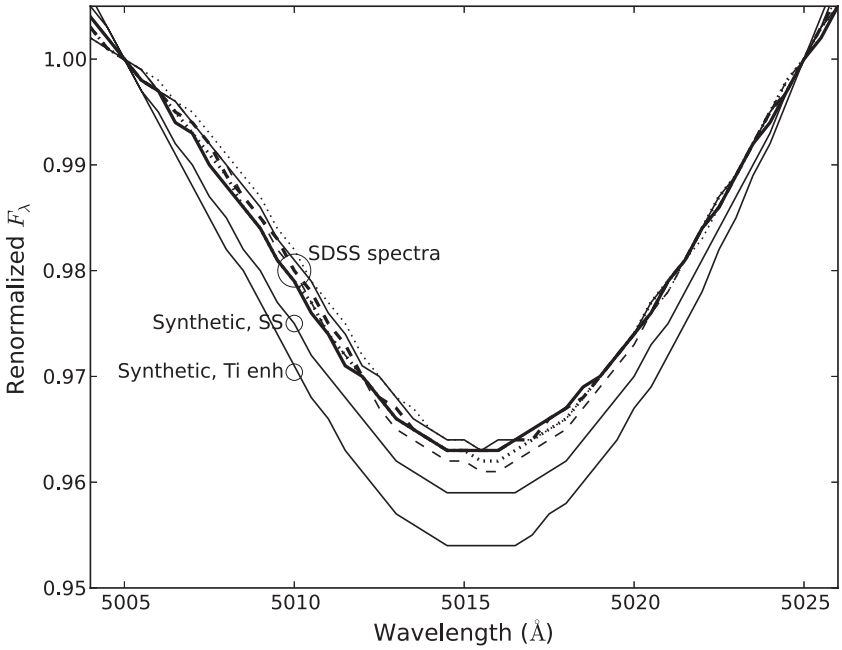

Figure 2. SDSS average galaxy spectra are shown in a spectral region expected to be sensitive to atomic Ti, along with scaled-solar (SS) and Ti-enhanced synthetic stellar population spectra. All spectra were smoothed to 300 km s^{-1} and renormalized to agree at nick points 5005 and 5025 Å. [Ti/R] = 0.3 for the Ti-enhanced spectrum. The velocity dispersions for the observed spectra are hard to see because they overplot each other, but they are: 95 km s^{-1} (thin dotted line), 127 km s^{-1} (thin dashed line), 152 km s^{-1} (thin solid line), 175 km s^{-1} (thick dotted line), 205 km s^{-1} (thick dashed line), and 260 km s^{-1} (thick solid line).

the unconstrained inversion program are therefore subject to noise and give [Sr/R] or [Al/R] values that are sometimes more than a factor of 10 away from the solar value. The "R" in the above notation stands for "any heavy element that is not being specifically called out." For example. it could be equated to uranium, if one desired. In any case, it scales with the solar abundance pattern. One should find, for example, that [Fe/H] = [Fe/R]+[R/H]. Indeed, for any element Q, [Q/H] = [Q/R]+[R/H]. Additionally, [Q/Fe] = [Q/R] − [Fe/R]. As always, square-bracket notation means base-10 logarithmic abundance relative to the solar value. Most of the results will be quoted as relative to Fe, but by this notation, [Fe/R] has meaning, whereas [Fe/Fe] does not.

The second way an element can give spurious results is if it is rather weak yet widespread in wavelength so that it affects many indices. Manganese, Co, Ni are like that. Iron is almost like that, but it affects the spectrum very strongly, not weakly. The third way is illustrated by the pair O and Ti. Increasing one or other of O or Ti will increase the strengths of TiO features, and TiO features carry a lot of weight in the spectrum, affecting many indices, so this pair of elements couples to one another strongly, compensating for each other along a predictable degeneracy axis.

However, Ti enjoys the luxury of providing some atomic transitions as well. In our synthetic spectra, the effects of 0.3 dex enhancement of Ti are clearly seen near 4296, 4533, and 5000 Å in the spectrum. However, the stacked SDSS spectra, when normalized to bracket the atomic Ti absorptions, show responses of confusing sense and also easily explainable by absorption from other species such as C or Fe. One example is show in Figure 2, where a blend of atomic Ti at 5007.21 Å and 5014.19 Å and some lesser lines contribute. In that example, the observed spectra show no coherent change with velocity dispersion, though using the synthetic spectra as guide, a 0.3 logarithmic enhancement of Ti abundance should clearly be visible. In other words, by spectral comparison, the atomic Ti shows no evidence for varying at all as a function of galaxian velocity dispersion.

This null result enables us to simplify the problem by one element, and for the most part we held Ti fixed at scaled-solar abundance. For purposes of this abundance-centered exercise, the ages and overall heavy metal abundances are mean values from assumed single-burst simple stellar populations and are not meant to be particularly realistic in terms of a true representation of the stellar populations within a given target galaxy. The age-metallicity degeneracy (Worthey 1994) remains in full play, decoupling from the process of finding element abundance ratios as described in Worthey (1994). The effects of metallicity compositeness on absorption feature strengths are probably detected in the far blue (Serven et al. 2011), but our spectra do not cover a large enough wavelength span to reach the NH 3360 feature. Inclusion of metallicity compositeness or swapping in different isochrone sets would have similar effects, namely, shifting zero points. The spans of the abundance shifts should remain almost invariant.

3. RESULTS

Sample results are illustrated in Figures 3–6. Galaxies are marked by alphanumeric codes for individual identification. The set of SDSS grand averages from Graves et al. (2007) begin with the letter "S" followed by the velocity dispersion of the bin. The galaxies from Serven (2010) are the NGC catalog numbers. Numbers in the 4000s are members of the Virgo Cluster. Elements not illustrated have been set to lockstep; for example, [Fe/R] = [Sr/R] = [Mn/R] = [Ti/R] = 0. In the present scheme, [M/H] is not necessarily the same as [R/H] due to the fact that the isochrones do not have flexible chemistry and do not vary as the chemical mix changes. [M/H] indicates

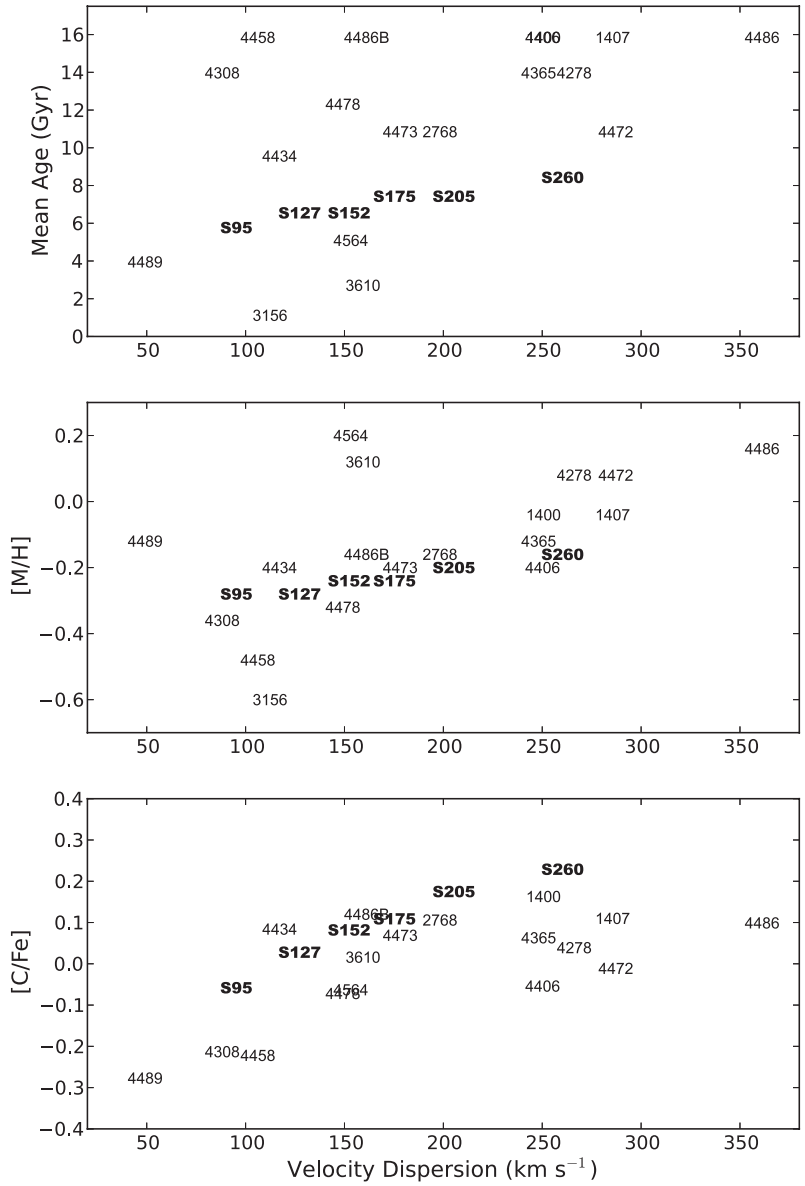

Figure 3. Assumed single-burst mean age, mean heavy-element abundance, and [C/Fe] as a function of velocity dispersion and as derived from one particular run of the inversion program with [Fe/H] set to lockstep with [M/H]. Four digit numerals indicate NGC numbers of galaxies in the Serven sample, while numerals following the letter "S" indicate SDSS grand-average galaxies of the indicated velocity dispersion. The six galaxies at age 16 Gyr have railed to the maximum allowed age. NGC 3156 is excluded in the [C/Fe] panel due to unreliable convergence.

the scaled-solar label on the best-fitting isochrone, as "Age" indicates the age label on the best-fitting isochrone.

The young age of NGC 3156, seen in Figure 3, around 1 Gyr, is a very robust age, but it means that the metallic features are quite weak, and the rest of the parameters for that galaxy are uncertain. Most of the individual galaxies fit about the same as or better than the SDSS average galaxies in terms of rms reproduction of all the indices by the final model. As is typical (Graves et al. 2009), Figure 3 shows a dearth of young, massive objects, and thus the average age increases at higher velocity dispersions. The dispersion in mean age for the individual galaxies is, by and large, real.

The abundance trends in Figures 3–6 are clearly increasing with velocity dispersion, especially [M/H], [C/Fe], [O/Fe], [Na/Fe], and [Si/Fe]. [M/H] equates to [R/H] and [Fe/H] for the illustrated inversion program run. When other elements are included, especially O, the [Mg/Fe] trend weakens somewhat compared with historical estimates such as Worthey et al. (1992). [N/Fe] and [Ba/Fe] also weakly rise, and [Ca/Fe] stands alone as weakly declining.

There is the appearance of a two-family bifurcation between SDSS and Serven samples in the [Si/Fe] trend of Figure 5. The [Si/Fe] is a relatively volatile one, resting on SiH molecular features in the blue that aren't captured terribly well by the indices and also are probably not secure in the synthetic spectra. Small systematic drifts in the input spectra can effect substantial changes in the inferred Si abundances. The same could be said for Ba.

4. DISCUSSION AND CONCLUSIONS

The uncertainty in the trends is the crucial question. It is clear that signal-to-noise ratio is not an issue. The uncertainties are a combination of systematic effects in the spectra and modeling

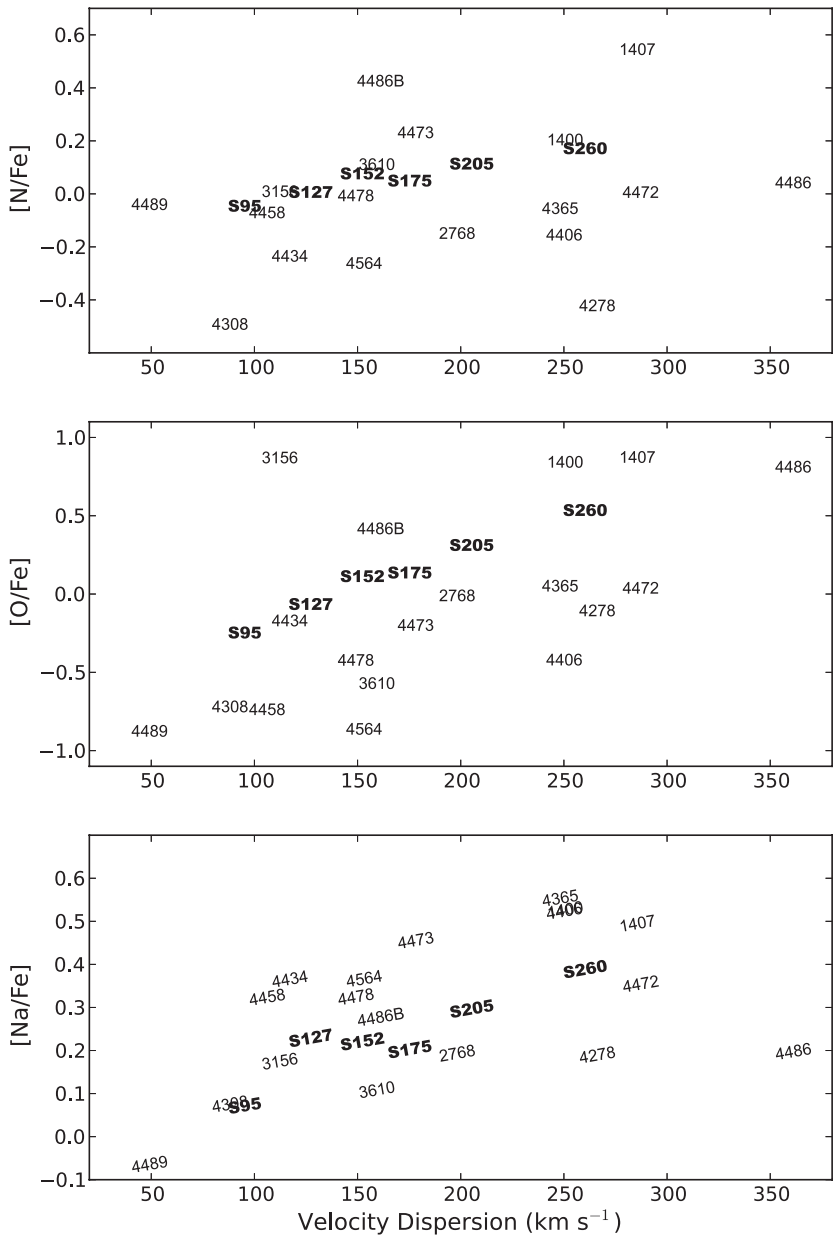

Figure 4. [N/Fe], [O/Fe], and [Na/Fe] as a function of velocity dispersion and as derived from one particular run of the inversion program with [Fe/H] set to lockstep with [M/H]. Four-digit numerals indicate NGC numbers of galaxies in the Serven sample, while numerals following the letter "S" indicate SDSS grand-average galaxies of the indicated velocity dispersion.

uncertainties. The inversion methods are also relatively untried. To gauge a scalable estimate of at least the modeling uncertainties, we added and subtracted elements from the list of things to be fit, making many permutations of the list and recording the inverted parameters. We included Ti several times, with the rule that O must be turned off during those runs.

Using the $\sigma = 260$ km s^{-1} average galaxy minus the $\sigma = 95$ km s^{-1} average galaxy as a convenient benchmark for estimating the range in the abundance parameters over the span of velocity dispersion, we collected the abundance results after the subsampling/permutation runs. We summarize the statistics in Table 1.

The standard deviations in Table 1 are, plausibly, overestimated compared to realistic uncertainties by our permutation process. For example, we never saw a negative [O/Fe] trend, although the standard deviation for [O/Fe] would imply that we should have. Clearly, some of the abundance trends are very secure, and they all seem significant except [Ca/Fe] and [Ba/Fe]. We do disagree with Conroy et al. (2013) that [Ba/Fe] decreases with velocity dispersion even though our barium-sensitive indices behave the same, observationally. We have no ironclad explanation for this at present, but we suspect that our largely empirical approach gives this work an edge in accuracy. Note that the present models reproduce the observed Ba index trends naturally, with no need to alter the Ba abundance by more than a few hundredths of a dex, and we speculate that this is mostly due to the correctness of the run of stellar index strengths that is based upon observed stars and not synthetic line lists. Parenthetically, Ba is a minor component of the absorption in the Ba indices; it is so named because of the maximized Ba sensitivity, not the total census of absorbers present in that spectral region. On the negative side, the individual galaxies have large scatter, and we are therefore not prepared to declare our mildly increasing Ba trend with velocity dispersion as significant.

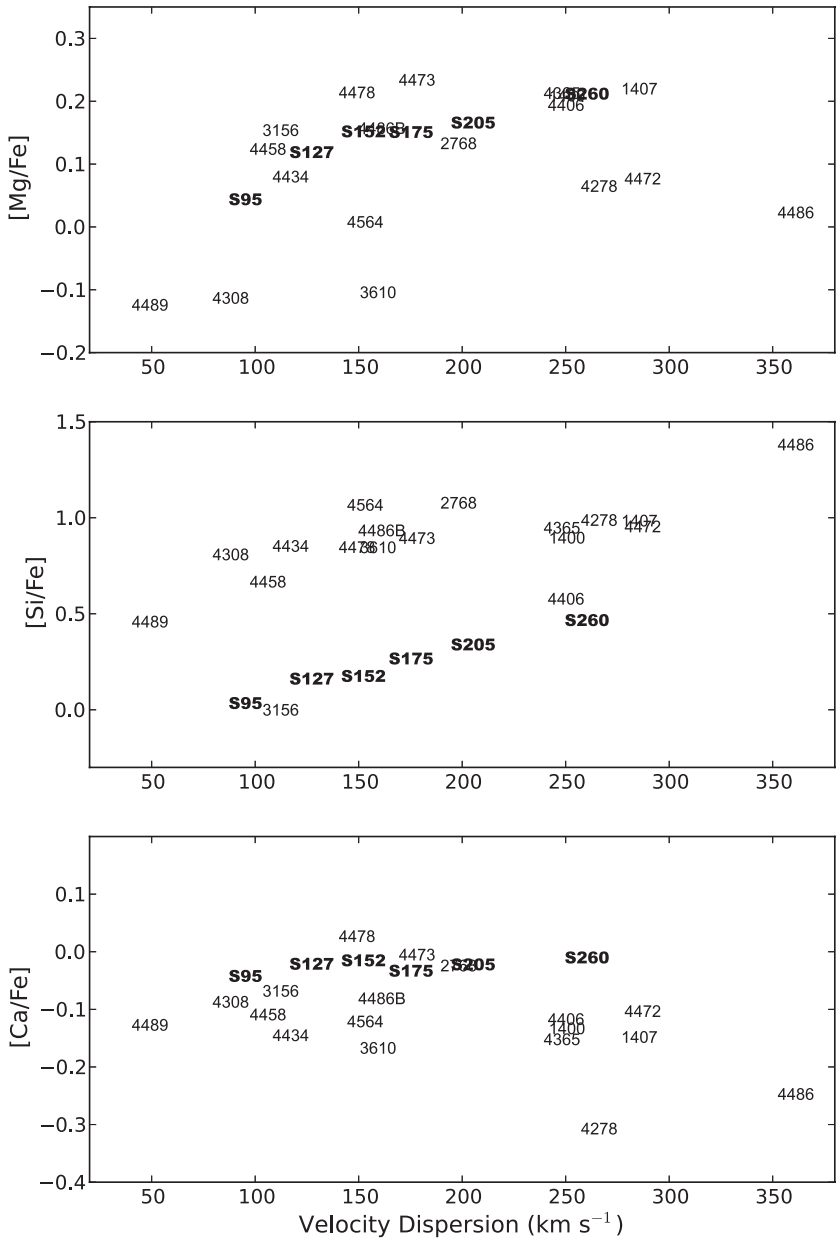

Figure 5. [Mg/Fe], [Si/Fe], and [Ca/Fe] as a function of velocity dispersion and as derived from one particular run of the inversion program with [Fe/H] set to lockstep with [M/H]. Four-digit numerals indicate NGC numbers of galaxies in the Serven sample, while numerals following the letter "S" indicate SDSS grand-average galaxies of the indicated velocity dispersion.

The scatter of individual galaxies itself is interesting if it can be shown to be in excess of the combination of observational and theoretical errors. The errors are not estimated well enough to use principle components analysis or similar techniques, but judging by the Table 1 standard deviations compared to the scatter in individual figures, and also tossing in an element of human judgment to exclude quantities that did not converge well, a list presents itself. [C/Fe] is a borderline case in that the relation with velocity dispersion looks approximately single-parameter in the sense that the dispersion about the relation is ∼0.1, about the same as the apparent combined observational and theoretical error from Table 1. We exclude O, Si, Ti, and Ba from the list because parameter convergence can be difficult. The remaining quantities, overall metallicity, [N/Fe], [Na/Fe], [Mg/Fe], [Ca/Fe], and [Fe/R], all show apparent cosmic scatter in the Serven (2010) data. Clearly, the chemical and star formation histories of individual galaxies can lead to different final abundance patterns. Excitingly, we are now entering an era where we can begin to measure such and are challenged to translate those measurements into individual histories for distant, unresolved galaxies.

As regards comparisons to previous work, Smith et al. (2009) are in general agreement with our Mg, C, and N trends, although the dependence of their [Ca/Fe] on velocity dispersion is rising and not flat. Johansson et al. (2012) find similar trends in all quantities they measure (C, N, O, Mg, Ti, Ca, Fe) within zero-point offsets of 0.1 dex or so, with the possible exception that we see an overall slightly positive slope for [Fe/R] and definite positive slope for [M/H], which together rather contradict their trendless [Fe/H] behavior versus velocity

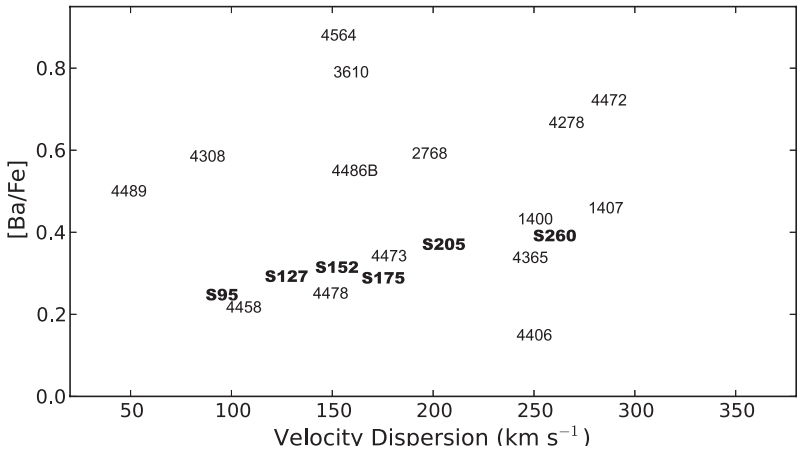

Figure 6. [Ba/Fe] as a function of velocity dispersion and as derived from one particular run of the inversion program with [Fe/H] set to lockstep with [M/H]. Four-digit numerals indicate NGC numbers of galaxies in the Serven sample, while numerals following the letter "S" indicate SDSS grand-average galaxies of the indicated velocity dispersion. NGC 3156 and NGC 4486 are excluded due to unsatisfactory convergence.

Table 1
Permutation Statistics

Quantity to Range	Mean of Range	Standard Deviation
Age (Gyr)	0.18	1.84
[M/H]	0.18	0.08
[C/Fe]	0.11	0.09
[N/Fe]	0.17	0.07
[O/Fe]	0.46	0.30
[Na/Fe]	0.29	0.03
[Mg/Fe]	0.15	0.03
[Si/Fe]	0.28	0.09
[Ca/Fe]	−0.01	0.03
[Fe/R]	0.07	0.06
[Ba/Fe]	0.04	0.09

Notes. The means are the ranges of each quantity, using the $\sigma = 260$ km s^{-1} average galaxy minus the $\sigma = 95$ km s^{-1} average galaxy. The statistics are then computed as permutations on the elements that are allowed to enter the fitting process of the inversion program.

dispersion. And, of course, our [O/Fe] is less than perfectly constrained and has a larger range than is realistic. There is another paper, Conroy et al. (2014), unrefereed as of this writing, in which other abundances are measured. Compared to that work, and restricted to SDSS averages, there is general broad agreement, and almost identical rising trends for [C/Fe], [N/Fe], and a flat trend for [Ca/Fe]. Our Si and O measurements are more wild as befits our stated errors and therefore also agree, though not with high fidelity. The increase we see with velocity dispersion in [Mg/Fe] is not quite as strong. As a final caution, in this work, little should be made of the inferred ages, since the experiment was not designed with accurate and properly multiparametric ages in mind.

Astrophysically, the trend among the alpha elements is rather fascinating. Ordered by mass, the alpha elements are O, Ne, Mg, Si, S, Ar, Ca, and Ti. We cannot measure Ne, S, or Ar due to lack of lines (Serven et al. 2005). Ca and Ti appear nearly locked to Fe in elliptical galaxies and are the heaviest alphas, while O, Mg, and Si show a strong parting of ways with Fe and are the lightest alphas. It is tempting based upon this correspondence to lump Ca and Ti with Type Ia supernovae and call the problem solved (cf. Pipino et al. 2009 especially in the case of Ca).

Current theoretical nucleosynthetic yield estimates seem too noisy to give much guidance as regards Ca and Ti (see discussion and references in Serven et al. 2005). Type Ia supernovae may contribute more than half of the Ca and Ti in the Sun. Thomas et al. (2011) support the idea that the heavier alpha elements have significant Type Ia components in the Milky Way. One empirical example is available in the Galactic bulge, in which all of the alpha elements seem to have positive but declining [X/Fe] except for possibly O, measurement of which seems to be slightly controversial, and Mg, which seems to linger at elevated levels even to high metallicity (Cunha & Smith 2006; McWilliam et al. 2008, 2010; Cescutti et al. 2009). The decline of alpha elements in the bulge may possibly be echoed by the most massive galaxy in our sample, NGC 4486, which lies rather lower than the trend in [C/Fe], [N/Fe], [Na/Fe], [Mg/Fe], and even [Ca/Fe] and possibly [O/Fe], seemingly unattenuated only for [Si/Fe]. The Ba measurement for NGC 4486 is too uncertain to call out specifically.

The elements that may have significant contributions from intermediate-mass stars through mass loss on the asymptotic giant branch include N manufactured during CNO cycle H fusion, C manufactured during He fusion, and neutron-capture elements such as Sr, which we cannot measure, and Ba, which we do. Intermediate-mass stars are $3\,M_\odot$ through $8\,M_\odot$ with a sweet spot for chemical enrichment happening around a $5\,M_\odot$ lifetime of about 200 Myr, that is, fairly short compared to what is most often contemplated as the Type Ia supernova enrichment timescale. On the other hand, if the *s*-process elements are more characterized by $\sim 3\,M_\odot$ stars, then the enrichment time pushes more toward 10^9 yr and becomes comparable, so it is quite possible that Ba enrichment will appear to be locked to Fe, but via coincidence, not via true commonality of enrichment source. Since elliptical galaxies are chemically evolved systems, it is not possible to separate primary enrichment (primordial supernovae) from secondary enrichment (after the creation of C, from which N can then be manufactured).

The abundance trends are presumably related to galaxy dynamics during formation. The interesting underlying context of the problem is that we observe abundance trends with galaxy mass. If mass drives the abundance trends, then the philosophical

conundrum presents itself: How does a galaxy know its final mass, in order to create the appropriate element mixture, before it is assembled? The obvious way is to invoke the idea that most of the galaxy formed all at once in a gaseous collapse, with star formation eventually truncated by supernova-driven winds, e.g., as modeled by Matteucci & Tornambe (1987). Unfortunately, this appealing mode of formation cannot be the dominant one, since, apparently, more than half of large early-type galaxies did not exist as recognizable analogs to modern elliptical galaxies until after $z = 1$ (Bell et al. 2004; Bundy et al. 2006; Faber et al. 2007; Ilbert et al. 2010). Furthermore, as might be inferred even from the present paper alone, individual galaxies can be quirky enough to scatter far from the average trend, implying possible strong ties between a hierarchical assembly formation history and the present-day abundance pattern.

But individualism cannot be wholly triumphant, since the average trend also exists, and theoreticians have been successful in matching many of the trends seen by parameterizing and varying quantities such as initial mass function, star formation rate or efficiency, wind parameters, Type Ia supernova timescale, Type II supernova yields, gaseous versus stellar (wet versus dry) merger patterns, dust content, and the character of gaseous infall (e.g., Bekki & Shioya 1998; Pipino & Matteucci 2004; Yates et al. 2013; Pipino et al. 2011; Tortora et al. 2013). Better observational material can only help these efforts toward understanding the inner workings of galaxy formation.

In summary, we have analyzed two sets of spectra for early-type galaxies in an attempt to pin down trends for O and Si for the first time in these systems, getting trends that agree by and large with previous Mg measurements, at least qualititatively. In addition to O and Si, we also measure abundances for C, N, Na, Mg, Ca, Fe, and Ba. Larger galaxies generally have a higher alpha element to iron peak ratio indicative of a higher ratio of Type II to Type Ia supernova products with the exception of the heaviest alpha elements, Ca and Ti, which seem to follow Fe more closely. The [Mg/Fe] trend is significant, but shows less range than past estimates. Elements that likely have significant contributions from intermediate-mass stars, namely, C, N, and Ba, also gain ground relative to Fe in massive galaxies at a modest level, with the Ba conclusion uncertain from our data alone.

In terms of surprises and conclusions that overturn established wisdom, there are none; the basic picture that it is mostly the Type II / Type Ia chemical signatures that drive the abundance trends is still a valid hypothesis. Two items are noteworthy, though currently apparently insoluble astrophysically. First, Ca and Ti appear to track Fe, and it would be lovely to know if those elements were Type Ia supernova products as Fe is, or if there is a progenitor mass dependence on the Ca and Ti enrichment. Second, the light elements C and N could have supernova contributions, and it would be lovely to know quantitatively what those might be as a function of star formation and chemical evolution timescales. Measuring Ba better may not solve this issue, as Ba can be made in the *r*-process as well (Sneden et al. 2003) and also may be manufactured on a timescale similar to Type Ia supernova products.

Finally, most element ratios seem to show cosmic scatter from galaxy to galaxy.

The authors would like to thank G. J. Graves, C. Conroy, R. L. Kurucz, J. A. Rose, and S. C. Trager for ongoing advice and warm collegiality, and an anonymous referee for helpful and insightful comments.

REFERENCES

Audouze, J., & Tinsley, B. M. 1976, ARA&A, 14, 43
Bekki, K., & Shioya, Y. 1998, ApJ, 497, 108
Bell, E. F., Wolf, C., Meisenheimer, K., et al. 2004, ApJ, 608, 752
Bensby, T., & Feltzing, S. 2006, MNRAS, 367, 1181
Bertelli, G., Bressan, A., Chiosi, C., Fagotto, F., & Nasi, E. 1994, A&AS, 106, 275
Bundy, K., Ellis, R. S., Conselice, C. J., et al. 2006, ApJ, 651, 120
Burbidge, E. M., Burbidge, G. R., Fowler, W. A., & Hoyle, F. 1957, RvMP, 29, 547
Busso, M., Gallino, R., & Wasserburg, G. J. 1999, ARA&A, 37, 239
Buzzoni, A., Chavez, M., Malagnini, M. L., & Morossi, C. 2001, PASP, 113, 1365
Cenarro, A. J., Gorgas, J., Vazdekis, A., Cardiel, N., & Peletier, R. F. 2003, MNRAS, 339, L12
Cenarro, A. J., Sánchez-Blázquez, P., Cardiel, N., & Gorgas, J. 2004, ApJL, 614, L101
Cescutti, G., Matteucci, F., McWilliam, A., & Chiappini, C. 2009, A&A, 505, 605
Chavez, M., Malagnini, M. L., & Morossi, C. 1995, ApJ, 440, 210
Chavez, M., Malagnini, M. L., & Morossi, C. 1996, ApJ, 471, 726
Chavez, M., Malagnini, M. L., & Morossi, C. 1997, A&AS, 126, 267
Chiappini, C., Matteucci, F., & Ballero, S. K. 2005, A&A, 437, 429
Chiappini, C., Romano, D., & Matteucci, F. 2003, MNRAS, 339, 63
Conroy, C., Graves, G., & van Dokkum, P. 2014, ApJ, 780, 33
Conroy, C., van Dokkum, P. G., & Graves, G. J. 2013, ApJL, 763, L25
Cunha, K., & Smith, V. V. 2006, ApJ, 651, 491
Davies, R. L., Sadler, E. M., & Peletier, R. F. 1993, MNRAS, 262, 650
Dotter, A., Chaboyer, B., Ferguson, J. W., et al. 2007, ApJ, 666, 403
Faber, S. M. 1973, ApJ, 179, 731
Faber, S. M., Willmer, C. N. A., Wolf, C., et al. 2007, ApJ, 665, 265
Franchini, M., Morossi, C., Di Marcantonio, P., et al. 2004a, ApJ, 601, 485
Franchini, M., Morossi, C., Di Marcantonio, P., et al. 2004b, ApJ, 613, 312
Franchini, M., Morossi, C., Di Marcantonio, P., et al. 2005, ApJ, 634, 1319
Graves, G. J., Faber, S. M., & Schiavon, R. P. 2009, ApJ, 698, 1590
Graves, G. J., Faber, S. M., Schiavon, R. P., & Yan, R. 2007, ApJ, 671, 243
Grevesse, N., & Sauval, A. J. 1998, SSRv, 85, 161
Gulati, R. K., Malagnini, M. L., & Morossi, C. 1993, ApJ, 413, 166
Ilbert, O., Salvato, M., Le Floc'h, E., et al. 2010, ApJ, 709, 644
Johansson, J., Thomas, D., & Maraston, C. 2012, MNRAS, 421, 1908
Kuntschner, H. 2000, MNRAS, 315, 184
Lee, H.-c., Worthey, G., Dotter, A., et al. 2009, ApJ, 694, 902
Matteucci, F. 1994, A&A, 288, 57
Matteucci, F., & Tornambe, A. 1987, A&A, 185, 51
Mattsson, L. 2010, A&A, 515, A68
McWilliam, A., Fulbright, J., & Rich, R. M. 2010, in IAU Symp. 265, Chemical Abundances in the Universe: Connecting First Stars to Planets, ed. K. Cunha, M. Spite, & B. Barbuy (Cambridge: Cambridge Univ. Press), 279
McWilliam, A., Matteucci, F., Ballero, S., et al. 2008, AJ, 136, 367
Paxton, B., Bildsten, L., Dotter, A., et al. 2011, ApJS, 192, 3
Peletier, R. F. 1989, PhD thesis, Univ. Groningen
Pipino, A., Chiappini, C., Graves, G., & Matteucci, F. 2009, MNRAS, 396, 1151
Pipino, A., Fan, X. L., Matteucci, F., et al. 2011, A&A, 525, A61
Pipino, A., & Matteucci, F. 2004, MNRAS, 347, 968
Prochaska, L. C., Rose, J. A., & Schiavon, R. P. 2005, AJ, 130, 2666
Sánchez-Blázquez, P., Peletier, R. F., Jiménez-Vicente, J., et al. 2006, MNRAS, 371, 703
Serven, J. 2010, PhD thesis, Washington State Univ.
Serven, J., Worthey, G., & Briley, M. M. 2005, ApJ, 627, 754
Serven, J., Worthey, G., Toloba, E., & Sánchez-Blázquez, P. 2011, AJ, 141, 184
Smith, R. J., Lucey, J. R., Hudson, M. J., & Bridges, T. J. 2009, MNRAS, 398, 119
Sneden, C., Cowan, J. J., Lawler, J. E., et al. 2003, ApJ, 591, 936
Thomas, D., Johansson, J., & Maraston, C. 2011, MNRAS, 412, 2199
Thomas, D., Maraston, C., & Bender, R. 2003, MNRAS, 343, 279
Toloba, E., Sánchez-Blázquez, P., Gorgas, J., & Gibson, B. K. 2009, ApJL, 691, L95
Tortora, C., Pipino, A., D'Ercole, A., Napolitano, N. R., & Matteucci, F. 2013, MNRAS, 435, 786
Trager, S. C., Worthey, G., Faber, S. M., Burstein, D., & Gonzalez, J. J. 1998, ApJS, 116, 1
Travaglio, C., Hillebrandt, W., Reinecke, M., & Thielemann, F.-K. 2004, A&A, 425, 1029
Tripicco, M. J., & Bell, R. A. 1995, AJ, 110, 3035
Tsujimoto, T., & Shigeyama, T. 2012, ApJL, 760, L38

Valdes, F., Gupta, R., Rose, J. A., Singh, H. P., & Bell, D. J. 2004, ApJS, 152, 251
Worthey, G. 1994, ApJS, 95, 107
Worthey, G. 1998, PASP, 110, 888
Worthey, G. 2004, AJ, 128, 2826
Worthey, G., & Collobert, M. 2003, ApJ, 586, 17
Worthey, G., Faber, S. M., & Gonzalez, J. J. 1992, ApJ, 398, 69
Worthey, G., Faber, S. M., Gonzalez, J. J., & Burstein, D. 1994, ApJS, 94, 687
Worthey, G., Ingermann, B. A., & Serven, J. 2011, ApJ, 729, 148
Worthey, G., & Lee, H.-c. 2011, ApJS, 193, 1
Worthey, G., & Ottaviani, D. L. 1997, ApJS, 111, 377
Yates, R. M., Henriques, B., Thomas, P. A., et al. 2013, MNRAS, 435, 3500